J Fluoresc (2007) 17:301–307
DOI 10.1007/s10895-007-0173-5

ORIGINAL PAPER

Mid-Infrared Emission Characteristic and Energy Transfer of Ho^{3+}-Doped Tellurite Glass Sensitized by Tm^{3+}

G. X. Chen · Q. Y. Zhang · G. F. Yang · Z. H. Jiang

Received: 19 November 2006 / Accepted: 14 February 2007 / Published online: 29 March 2007

Abstract We report on 2.0-μm emission characteristic and energy transfer of Ho^{3+}-doped tellurite glass sensitized by Tm^{3+} upon excitation of a conventional 808 nm laser diode. The Judd-Ofelt strength parameters, spontaneous radiative transition probabilities and radiative lifetime of Ho^{3+} have been calculated from the absorption spectra by using the Judd-Ofelt theory. Significant enhancement of 2.0-μm emission of Ho^{3+} has been observed with increasing Tm^{3+} doping up to 0.7 mol%. The energy transfer coefficient of the forward $Tm^{3+} \rightarrow Ho^{3+}$ is approximately 17 times larger than that of the backward $Tm^{3+} \leftarrow Ho^{3+}$ energy transfer. Our result indicates that the maximum gain of 2.0-μm emission, assigned to the transition of $^5I_7 \rightarrow {}^5I_8$ of Ho^{3+}, might be achieved from the tellurite glass at the concentration of 0.5 mol% of Tm_2O_3 and 0.15 mol% of Ho_2O_3. The high gain coefficient and quantum efficiency (1.16) along with the large value of the product of the stimulated emission cross-section and the measured radiative lifetime (4.12×10^{-27} m^2s) of the Ho^{3+}/Tm^{3+}-codoped tellurite glasses might find potential applications in efficient 2.0-μm laser.

Keywords Mid-infrared laser · Fluorescence · Energy transfer · Gain · Tellurite glass

Introduction

The mid-infrared (mid-IR) lasers operating at the range of 2.0–3.0 μm and beyond provide potential for application in laser medicine surgery, remote chemical sensing, eye-safe laser radar, the monitoring of atmospheric pollutions, high resolution spectroscopy of low pressure gasses [1–6]. Ever since Johnson [7] has reported the first laser action at 2.0 μm from Ho^{3+} doped $CaWO_4$ crystal in 1962, an intense level of research activity has been focusing on measuring the spectroscopic and lasing properties of Ho^{3+} doped various crystals and glasses [8–10].

Tellurite glasses exhibit high linear and nonlinear refractive indices, good resistance to corrosion, high mechanical stabilitiy and low cut-off phonon energy of around 750 cm^{-1}. Moreover, the transmission range of tellurite glasses extends into the mid-IR up to about 5 μm and it has good capacity to accept lanthanide dopants. The low phonon energy and wide transmission range of tellurite glasses allow the observation of rare-earth ions doped lasers emissions in a large optical range. These features, coupled with good resistance to corrosion and high mechanical stabilitiy, make tellurite glasses become promising host for mid-IR lasers at 2.0-μm wavelength.

In this article, we report on 2.0-μm emission characteristic and energy transfer of Ho^{3+}-doped TeO_2-WO_3-ZnO tellurite glass sensitized by Tm^{3+} upon excitation of a conventional 808 nm laser diode (LD). Effect of Tm^{3+} dopant on the fluorescence properties of 2.0-μm wavelength from Ho^{3+} has been investigated.

Experimental procedures

TeO_2-based glasses with the molar compositions of $70TeO_2$-$20WO_3$-10ZnO codoped with 0.3 mol% Ho_2O_3 and x mol% Tm_2O_3 ($x = 0$, 0.1, 0.3, 0.5 and 0.7), and $70TeO_2$-$20WO_3$-10ZnO codoped with 0.5 mol% Tm_2O_3 and y mol% Ho_2O_3 ($y = 0$, 0.01, 0.05, 0.10 and 0.15) were prepared by

G. X. Chen · Q. Y. Zhang (✉) · G. F. Yang · Z. H. Jiang
Key Lab of Specially Function Materials of Ministry of Education, and Institute of Optical Communication Materials, South China University of Technology, Guangzhou 510641, P. R. China
e-mail: qyzhang@scut.edu.cn

using reagent-grade TeO_2 (99.99%), WO_3 (99.99%), ZnO (99.99%), Ho_2O_3 (99.99%) and Tm_2O_3(99.99%). Batch materials of 15 g were mixed well and melted at about 850°C for 20 minute with a platinum crucible. Melts were thermally quenched by casting the melt into a preheated stainless steel mold, and then annealed at a temperature close to the vitreous transition temperature for two hours before ramping down to room temperature. All the obtained samples were cut into specimens of 10 mm × 10 mm × 2 mm and optically polished for the measurement of the absorption and emission spectra.

Absorption spectra of rare-earth doped samples were determined by a Perkin-Elmer Lambda 900/UV/VIS/NIR spectrophotometer in the spectral range of 400–2300 nm at room temperature. The fluorescence spectra in the range of 1600–2200 nm were obtained by using a computer-controlled TRIAX 320 fluorescence spectrometer (Jobin-Yvnon Corp.) with a 808 nm LD as pump source.

Results and discussion

Spectroscopy characteristics and Judd-Ofelt analysis

Figure 1 shows the room temperature absorption spectra in the UV-visible and IR regions of Ho^{3+}-doped tellurite glass sensitized by Tm^{3+}. The absorption bands represent the transitions from the ground state to the excited states of 4f configuration of Tm^{3+} and Ho^{3+}, respectively. Owing to the strong intrinsic bandgap absorption located at 420 nm in the host glasses, absorption from Ho^{3+} cannot be clearly identified below 420 nm. It is worthwhile to mention that the amplitude of the band near 794 nm is no less than those of the other three observed bands of Tm^{3+}, which indicates that Tm^{3+} ion in the glass can be excited efficiently by 808 nm LD. Figure 2 shows the schematic energy levels of Tm^{3+} and

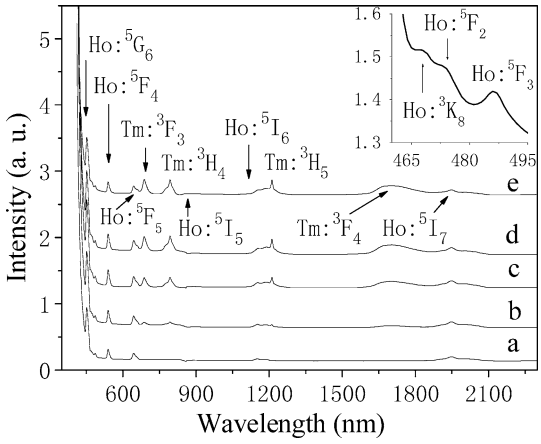

Fig. 1 Absorption spectra of the TeO_2-WO_3-ZnO glasses containing (a) 0, (b) 0.1, (c) 0.3, (d) 0.5 and (e) 0.7 mol% Tm_2O_3 with a fixed Ho_2O_3 concentration of 0.3 mol%. Inset shows the amplification of the absorption spectra curves in the range 460–500 nm

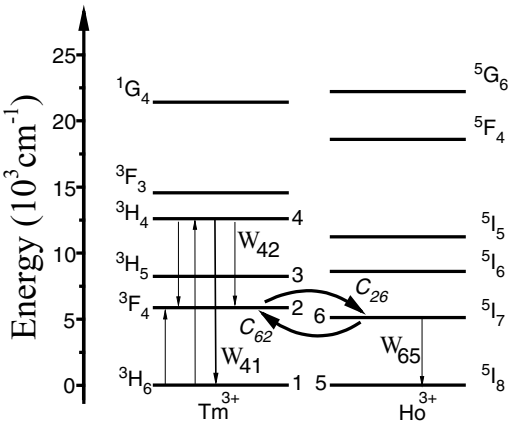

Fig. 2 Schematic energy levels diagram of Tm^{3+} and Ho^{3+} in TeO_2-WO_3-ZnO glass under excitation of 808 nm LD

Ho^{3+} identified from the absorption spectra of TeO_2-based glasses. The locations of the energy levels were very similar to those reported previously for chalcogenide [6], tellurite [11] and fluoride [2] glass hosts.

The Judd-Ofelt analyses [12, 13] were applied using the experimental oscillator strengths of the absorption bands obtained from absorption spectrum. The Judd-Ofelt intensity parameters, Ω_t ($t = 2, 4, 6$), can be figured out utilizing the reduced matrix elements of the unit tensor operators provided by Rukmini et al. [14]. The comparisons of Ω_t in various Ho^{3+}-doped glass hosts are shown in Table 1. Generally, Ω_2 is closely related to the ligand symmetry of host material and the orderliness of structure. It is hypersensitive to the change of compositions in materials. The Ω_t parameters follow the trend $\Omega_2 > \Omega_4 > \Omega_6$ in tellurite glass. Ω_4, and Ω_6 are related to the covalence of the lattice site of rare earth ions, which can be adjusted by the composition or structure of the glass hosts. The larger the value of Ω_6, the weaker will be the covalence between rare earth ions and anions. It should be mentioned that the Ω_6 value in tellurite glass (this work) is only less than those of fluorophosphates and ZnBS glass, but

Table 1 The Judd-Ofelt intensity parameters of Ho^{3+} doped various glasses

Glass	Ω_2	Ω_4	Ω_6	Ω_4/Ω_6
ZnBS [14]	22.42	5.19	12.33	0.429
Fluoride [14]	2.43	1.67	1.84	0.908
PbO-Bi_2O_3-Ga_2O_3 [15]	4.77	2.18	1.22	1.7869
Fluorophosphate [2]	2.10	3.5	2.5	1.4
Germinate [2]	3.30	1.14	0.17	0.0671
PbO-SiO_2 · [14]	5.20	1.80	1.20	1.5
Phosphate [14]	5.60	2.72	1.87	1.4545
$YAlO_3$ [16]	1.82	2.38	1.53	1.556
$Ge_{30}As_{10}S_{60}$ [15]	6.98	2.53	0.78	3.2436
$NaTeO_2$ [16]	6.92	2.81	1.42	1.979
Tellurite[This Work]	5.26	2.28	2.18	1.0459

Table 2 Electric dipole linestrengths (S_{ed}), radiative transition probabilities ($A_{ed} + A_{md}$), total radiative transition probabilities (A_r), branching ratios (β) and radiative lifetime (τ_{rad}) for fluorescence levels of Ho^{3+} ions in tellurite glass

SLJ	S′L′J	Energy (cm^{-1})	S_{ed} (10^{-20} cm^2)	$A_{ed} + A_{md}$(s^{-1})	β
$^5I_7 \rightarrow$	$^5I_8$	5128	3.309064	201 + 56.5	1.00
		$A_r(^5I_7) = 257.5\ s^{-1}$ $\tau_{rad}(^5I_7) = 3891$ us			
$^5I_6 \rightarrow$	$^5I_8$	8620	1.422492	472	0.85
	$5I_7$	3492	2.253802	50 + 30.43	0.15
		$A_r(^5I_6) = 552.43\ s^{-1}$ $\tau_{rad}(^5I_6) = 1809$ us			
$^5I_5 \rightarrow$	$^5I_8$	11236	0.199865	174	0.39
	$^5I_7$	6108	1.70382	238	0.53
	$^5I_6$	2616	1.773691	19 + 15.034	0.08
		$A_r(^5I_5) = 446.03\ s^{-1}$ $\tau_{rad}(^5I_5) = 2241$ us			
$^5F_5 \rightarrow$	$^5I_8$	15480	2.25566	5128	0.77
	$^5I_7$	10352	1.846296	1255	0.19
	$^5I_6$	6860	1.323036	262	0.04
	$^5I_5$	4244	0.415881	19	0.00
		$A_r(^5F_5) = 6664 s^{-1}$ $\tau_{rad}(^5F_5) = 150$ us			
$^5F_4 \rightarrow$	$^5I_8$	18553	1.989327	9516	0.81
	$^5I_7$	13425	0.619486	1123	0.09
	$^5I_6$	9933	1.057586	776	0.07
	$^5I_5$	7317	1.239247	364	0.03
	$^5F_5$	3073	1.351096	29 + 10.485	0.00
		$A_r(^5F_4) = 11818.49\ s^{-1}$ $\tau_{rad}(^5F_4) = 87$ us			
$^5F_3 \rightarrow$	$^5I_8$	20576	0.634095	5320	0.48
	$^5I_7$	15448	1.123317	3988	0.36
	$^5I_6$	11956	0.651673	1073	0.10
	$^5I_5$	9340	0.657667	516	0.05
	$^5F_5$	5096	0.598809	76	0.01
	$^5F_4$	2023	0.785002	6 + 5.463	0.00
		$A_r(^5F_3) = 10984.46\ s^{-1}$ $\tau_{rad}(^5F_3) = 91$ us			
$^5G_5 \rightarrow$	$^5I_8$	24200	1.503502	13059	0.40
	$^5I_7$	19042	3.44781	14589	0.45
	$^5I_6$	15510	1.364074	3119	0.68
	$^5I_5$	12932	0.312998	415	0.09
	$^5F_5$	8566	2.202877	849	0.18
	$^5F_4$	5383	1.868582	179	0.04
	$^5F_3$	3431	1.358555	34	0.01
	$^5F_2$	2840	0.448878	6	0.00
	$^5K_8$	2687	0.024813	0	0.00
	$^5G_6$	1721	1.505544	5 + 0.98932	0.00
		$A_r(^5G_5) = 32250.99\ s^{-1}$ $\tau_{rad}(^5G_5) = 31$ us			

larger than those of the others. Since the $^5I_7 \rightarrow {}^5I_8$ transition of Ho^{3+} is mainly affected by Ω_6 and A_r (spontaneous emission probabilities) is proportional to Ω_6 [2], the tellurite glass should have high A_r value for the $^5I_7 \rightarrow {}^5I_8$ transition of Ho^{3+}. It is interesting to note that the Ω_4/Ω_6 ratio is found to be about one in the glass and fluoride glass. Table 2 represents the (A_r), fluorescence branching ratio (β) and radiative lifetime (τ_r) of different levels of Ho^{3+} ions which were calculated using the calculated Judd-Ofelt intensity parameters. The results show that the values of τ_r and A_r of the $^5I_7$ level

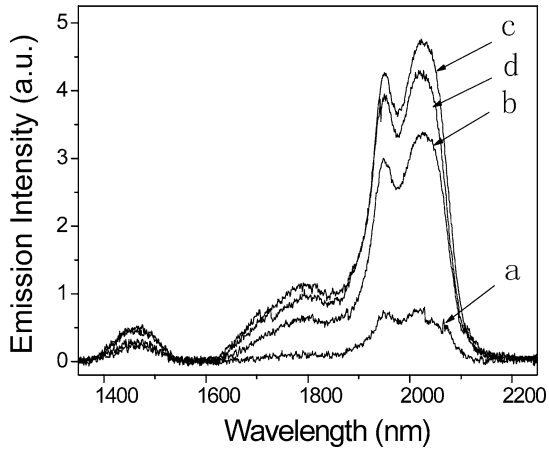

Fig. 3 Fluorescence spectra of the TeO_2-WO_3-ZnO glasses containing (a) 0.1, (b) 0.3, (c) 0.5 and (d) 0.7 mol% Tm_2O_3 with a fixed Ho_2O_3 concentration of 0.3 mol% upon excitation at 808 nm LD

of Ho^{3+} are about 3.9 ms and 257.5 s^{-1}, respectively. These values are comparable to that found by Singh [17].

Figure 3 shows the fluorescence spectra of Ho^{3+}-doped tellurite glass sensitized by Tm^{3+} in the range of 1400–2200 nm under excitation of 808 nm LD at the room temperature. The emission peaks at 1.47-, 1.8- and 2.0-μm are assigned to the transitions of Tm^{3+}: $^3H_4 \rightarrow {}^3F_4$, Tm^{3+}: $^3F_4 \rightarrow {}^3H_6$ and Ho^{3+}: $^5I_7 \rightarrow {}^5I_8$, respectively. It can be clearly seen that the emission intensity of the peak at 1.47-μm changes slightly with Tm_2O_3 concentration. The emission intensity of the peak at 1.8-μm increases with increasing Tm_2O_3 concentration while that of the peak at 2.0-μm increases significantly. However, there is no emission band at around 2.0-μm in the Tm_2O_3 singly doped glass. These indicate that the 2.0-μm emission of Ho^{3+} can only originate from energy transfer (ET) of Tm^{3+} to Ho^{3+} ion because Ho^{3+} ion has no absorption band at around 808 nm. Therefore, it is expected that an efficient ET process from Tm^{3+} to Ho^{3+} will play an important role in Tm^{3+}/Ho^{3+}-codoped glasses pumped by 808 nm LD. In addition, a maximum of the emission intensity of 2.0-μm emission is observed for a Tm_2O_3 content of about 0.5 mol%.

Gain spectra characteristics

Figure 4 shows the absorption cross-section and stimulated emission cross-section of Ho^{3+} for the 2.0-μm transition in the TeO_2-WO_3-ZnO glasses. The absorption cross-section, $\sigma_a(\lambda)$, was determined from the absorption spectra by using Beer-Lambert equation [3]

$$\sigma_a(\lambda) = \frac{2.303 \log(I_0/I)}{Nl} \quad (1)$$

where I_0 and I are the intensities of incident and transmitted light, respectively, N is the concentration of Ho^{3+},

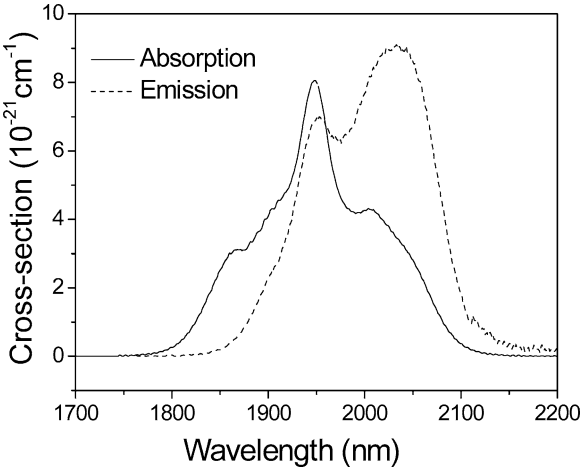

Fig. 4 Absorption cross-sections and the derived emission cross-sections of TeO_2-WO_3-ZnO glasses doped with 0.5 mol% Tm_2O_3 and 0.3 mol% Ho_2O_3

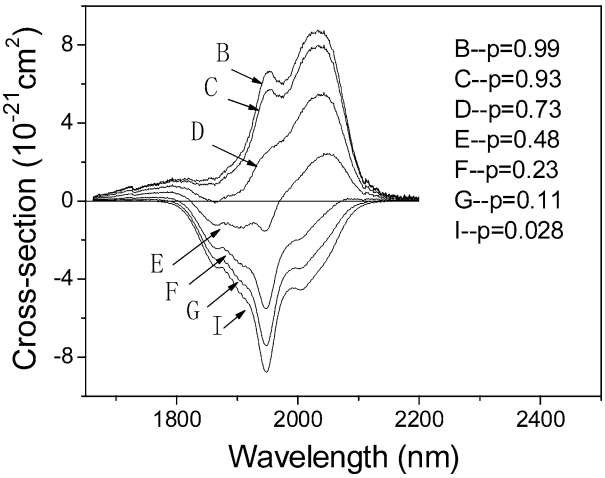

Fig. 5 Gain spectra of Ho^{3+} near the 2.0 μm wavelength region in Tm^{3+}/Ho^{3+}-codoped TeO_2-WO_3-ZnO glass

and l is the thickness of the sample. The absorption cross-section of Ho^{3+}: $^5I_8 \rightarrow {}^5I_7$ transition had a maximum of 8.06×10^{-21} cm^2 at 1948 nm. The stimulated emission cross-section, $\sigma_e(\lambda)$, was calculated from the fluorescence spectra utilizing Fuchtbauer-Ladenburg equation [18]

$$\sigma_e(\lambda) = \frac{\lambda^4}{8\pi c n^2} A_r g(\lambda) \tag{2}$$

where $g(\lambda)$ is the normalized line-shaped function obtained from the measured fluorescence spectra, c is the speed of light, n is the refractive index. The emission cross-section of Ho^{3+}: $^5I_7 \rightarrow {}^5I_8$ transition had a maximum of 9.15×10^{-21} cm^2 at 2027 nm. This value is almost one time larger than that of gallate-bismuth-lead glass (5.44×10^{-21} cm^2) [3] or fluorite glass (5.3×10^{-21} cm^2) [2], but less than that of chalcogenide glass (15.4×10^{-21} cm^2) [6]. The larger absorption and emission cross-section of Ho^{3+} is mainly due to the high refractive index of glass matrix [4] and high spontaneous transition probability. This provides advantages for efficient laser output.

Figure 5 presents the gain spectra of Ho^{3+} near the 2.0-μm wavelength region in Tm^{3+}/Ho^{3+}-codoped samples. The calculated gain coefficients could be determined by using: $G(\lambda) = n(^5I_7)\sigma_e(\lambda) - n(^5I_8)\sigma_a(\lambda)$ [3], where $n(^5I_7)$ and $n(^5I_8)$ are the electron population densities of the $^5I_7$ and $^5I_8$ levels in Ho^{3+}, respectively. If electrons in Ho^{3+} are only in either the $^5I_7$ or $^5I_8$ state, we can simplify the equation to $G(\lambda) = N[p\sigma_e(\lambda) - (1-p)\sigma_a(\lambda)]$, where N is the concentration of Ho^{3+}, and p is the population inversion rate. The values of $G(\lambda)/N$ could be calculated by assuming different p values. The gain spectra characteristics (Fig. 5) are similar to those of fluorescence spectra in the Ho^{3+}-doped TeO_2-WO_3-ZnO glasses sensitized by Tm^{3+}. The peak wavelength at which the highest gain of 2.0-μm emission occurs is centered at 2027 nm along with a shoulder centered at 1948 nm. When $p > 0.93$, the shape of gain spectrum resembles that of fluorescence spectrum of Ho^{3+} near the 2.0-μm wavelength region. When $0.23 < p < 0.93$, the value of gain near the 1948 nm wavelength region decreases rapidly while that near the 2.0-μm wavelength region is relatively reduced slowly. With the reduction of the value of p (namely, with decreasing with population inversion for Tm^{3+}/Ho^{3+} co-doped system), the peak wavelength at which the highest gain of 2.0-μm emission occurs shifts to longer wavelengths. This phenomenon is a typical characteristic of the quasi-three-level laser. Since the gain coefficient is directly proportional to the quantum efficiency of the specific transition (Refs. [3, 19]), indicating the glass studied should has a high quantum efficiency.

Table 3 represents the results of calculated quantum efficiencies (η), peak emission cross-section (σ_e), measured peak wavelength (λ_p) of the emission spectrum and the product ($\sigma_e \times \tau_m$) of the peak emission cross-section and the upper state measured lifetime (τ_m) in various Ho^{3+}-doped glasses. High quantum efficiency is one major parameter of evaluating laser glasses. Quantum efficiency can be expressed as [1, 2] $\eta = \tau_m/\tau_r$. Quantum efficiency of the emitting level is strongly affected by the phonon energy of glass hosts [1, 2]. Generally, the lower the phonon energy of glass hosts, the higher the quantum efficiency of the emitting level. Nevertheless, the fluoride and heavy metal oxides such as gallate-bismuth-lead glass [20] with lower phonon energy have high quantum efficiency. $\sigma_e \times \tau_m$ is another major parameter of evaluating laser glass. Especially, it plays the key role for cw operation [1]. It is interesting to note from Table 3 that the values of the quantum efficiencies in fluoride and tellurite glasses are much higher than those in the other oxide glasses and the value of $\sigma_e \times \tau_m$ in fluoride

Table 3 Spectroscopic properties of various Ho^{3+} doped glasses

	λ_p/nm	N/wt%	A_r/s^{-1}	τ_m/ms	$\sigma_e/10^{-20}$ cm^{-2}	η	$\sigma_e \times \tau_m/10^{-27}$ m^{2}s
Fluoride [2]	2035	2	58.07	26.7	0.53	1.55	14.15
Gallate [2]	2055	2	69.53	8.2	0.38	0.57	3.12
Fluorophosphate [2]	2035	2	90.42	5.6	0.79	0.651	4.42
Silicate [2]	2040	2	61.65	0.32	0.70	0.02	0.22
Tellurite	2027	2	257.5	4.5	0.915	1.16	4.12

Note. λ_p is measured peak wavelength, N is the dopant concentration, σ_e is the peak emission cross-section.

glass is the largest while that in silicate with high phonon energy is the lowest. The values of $\sigma_e \times \tau_m$ in tellurite, gallate and fluorophosphate glasses are almost equal. Although the measured lifetime (4.5 ms) [21] of the level $^5I_7$ of Ho^{3+} in tellurite glass is less than that in fluoride glass, the values of A_r and σ_e of the level $^5I_7 \rightarrow {}^5I_8$ transition of Ho^{3+} in tellurite glass are larger than those in fluoride glass. In a word, excluding fluoride glass, tellurite glass is superior to the other oxide glasses according to the values of η and $\sigma_e \times \tau_m$ (see Table 3). Therefore, we expect that tellurite glass will become an important host material of Ho^{3+} doped laser.

Cross-relaxation rate of Tm^{3+} ions and energy transfer analysis

There are at least two energy transfer processes in the Ho^{3+}-doped tellurite glass sensitized by Tm^{3+} upon excitation of 808 nm (LD). One is spatial energy transfer among Tm^{3+} ions followed by the cross-relaxation of $^3H_6(Tm^{3+}) + {}^3H_4(Tm^{3+}) \rightarrow {}^3F_4(Tm^{3+}) + {}^3F_4(Tm^{3+})$ that can improve pump quantum efficiency. Another process is resonant energy transfer from the $^3H_4(Tm^{3+})$ level to the $^5I_7(Ho^{3+})$ level that enhances 2.0-μm emission. The cross-relaxation rate (W_{CR}) can be calculated from the measured and calculated fluorescence lifetime of the $^3H_4(Tm^3)$ level by using Eq. (3). Because the phonon energy of tellurite glass ($\sim$750 cm^{-1}) is small compared to the energy separation of 4360 cm^{-1} between the level $^3H_4$ and $^3H_5$ of Tm^{3+} ions, the multiphonon relaxation rate (W_{MP}) is negligibly small. Then, the cross-relaxation rate can be simplified as Eq. (4).

$$\frac{1}{\tau_m} = \frac{1}{\tau_r} + W_{MP} + W_{CR} \tag{3}$$

$$W_{CR} \cong \frac{1}{\tau_m} - \frac{1}{\tau_r} \tag{4}$$

The result of calculating cross-relaxation rate among Tm^{3+} ions is shown in Table 4.

It is necessary to apply two assumptions to analyze the process of the energy transfer from Tm^{3+} to Ho^{3+} before utilizing a simple model in Fig. 2. First, only the lowest three energy levels of Tm^{3+} beside the $^3H_5$ level are considered due to the fast multiphonon decay from $^3H_5$ to $^3F_4$ level. Second, because of the low excitation rate from the $^5I_7$ to $^5F_4$, $^5S_2$ level, the upconversion related with the $^5I_7(Ho^{3+})$ level is so weak that only the lowest two levels of Ho^{3+} are considered. The rate equations are derived from Shin et al. [3].

$$\frac{dn_1}{dt} = -\phi_{808}\sigma_{Tm}n_1 - Rn_4n_1 + W_{41}n_4 + C_{26}n_2n_5 - C_{62}n_1n_6 + \frac{n_2}{\tau_2} \tag{5}$$

$$\frac{dn_2}{dt} = 2Rn_4n_1 + W_{42}n_4 - C_{26}n_2n_5 + C_{62}n_1n_6 - \frac{n_2}{\tau_2} \tag{6}$$

$$\frac{dn_4}{dt} = \phi_{808}\sigma_{Tm}n_1 - Rn_4n_1 - \frac{n_4}{\tau_4} \tag{7}$$

$$n_1 + n_2 + n_4 = n_{Tm} \tag{8}$$

$$\frac{dn_5}{dt} = -C_{26}n_2n_5 + C_{62}n_1n_6 + \frac{n_6}{\tau_6} \tag{9}$$

$$\frac{dn_6}{dt} = C_{26}n_2n_5 - C_{62}n_1n_6 - \frac{n_6}{\tau_6} \tag{10}$$

$$n_5 + n_6 = n_{Ho} \tag{11}$$

where ϕ_{808} and σ_{TM} are the flux of the incident pump photons and the absorption cross-section of Tm^{3+}, respectively. C_{ij} and W_{ij} are the energy transfer coefficient and rate from i to j energy level transition, respectively. n_i and τ_i are the electron population and lifetime of the i level, respectively. n_{Tm} and n_{Ho} are the total concentration of Tm^{3+} and Ho^{3+}, respectively. $R(W_{CR}/n_{Tm})$ is the cross-relaxation coefficient of

Table 4 Initial conditions used for the calculation of the rate equations (5) to (11)

Parameter	Value	Parameter	Value
$\emptyset_{808}$	1.706×10^{21}	σ_{Tm}(cm^2)	6.83×10^{-21}
W_{CR}	4367	τ_4(us) [22]	294.12
$W_{41}(s^{-1})$ [22]	3100	$W_{42}(s^{-1})$ [22]	300

Table 5 The calculated energy transfer coefficients C_{26} and C_{26} in Ho^{3+}-doped tellurite glass sensitized by Tm^{3+} upon excitation of 808 nm laser diode

Tm_2O_3 (mol%)	Ho_2O_3 (mol%)	C_{26} ($\times 10^{-17}$ cm^3/s)	C_{62} ($\times 10^{-17}$ cm^3/s)
0.5	0.15	32.6	1.58
0.5	0.1	31.8	1.63
0.5	0.05	30.8	1.61
0.5	0.01	29.3	1.55

Tm^{3+}. The initial conditions were $n_1(0) = n_{Tm}$, $n_2(0) = 0$, $n_4(4) = 0$, $n_5(0) = n_{Ho}$, $n_6(0) = 0$, $\tau_2 = 0.754$ ms [23], $\tau_6 = 3.9$ ms. The other parameters used in the rate equations are also listed in Table 4.

Table 5 shows the forward $Tm^{3+} \rightarrow Ho^{3+}$ energy transfer coefficient C_{26}, and vice versa C_{62} in Ho^{3+}-doped samples sensitized by Tm^{3+} upon excitation of 808 nm LD. Energy transfer coefficient C_{ij} can not be directly solved because it is multiplied by the same terms in the simultaneous equations. Another set of equations is needed. It can be obtained by exciting Ho^{3+} from ground state $^5I_8$ to upper level $^5I_7$ using a 900 nm excitation source. However, there is a strong energy transfer from Ho^{3+} to Tm^{3+} which is too complicated to analyze. Therefore, energy transfer coefficient C_{ij} will be indirectly solved by utilizing iterative method [3]. From Table 5, we can observe that the forward energy coefficient C_{26} (Tm^{3+}: $^3F_4 \rightarrow Ho^{3+}$: $^5I_7$) is about 17 times larger than the backward energy coefficient C_{62} (Tm^{3+}: $^3F_4 \leftarrow Ho^{3+}$: $^5I_7$).

Figure 6 shows the dependence of electron population densities of different levels of Tm^{3+} and Ho^{3+} ions on time in the TeO_2-WO_3-ZnO glasses. Electron population densities of different levels were obtained by numerically solving the rate equations from Table 4, Table 5 and the initial values of different levels described above using the Runge-Kutta method [24, 25]. After exponentially increasing or decreasing for a certain time, the electron population densities of different levels trend to a steady state.

Considering the unchange of the electron population densities of different levels when all energy levels are in steady state, the electron population densities of $^5I_7$ and $^5I_8$ levels of Ho^{3+} can be directly read out. The gain coefficients at 2027 nm for tellurite glasses doped with 0.5 mol% Tm_2O_3 and various concentration of Ho_2O_3 were calculated using the gain coefficients expression mentioned above and the results were shown in Fig. 7. Gain coefficient increases with increasing pump power intensity. Although gain coefficient can be obtained with small pump power intensity when the concentration of Ho_2O_3 is low, it increases very slowly with rapidly increasing pump power intensity. On the other hand, gain coefficient can be achieved only at relatively larger pump power intensity when the concentration of Ho_2O_3 is high, but it increases abruptly with increasing pump power

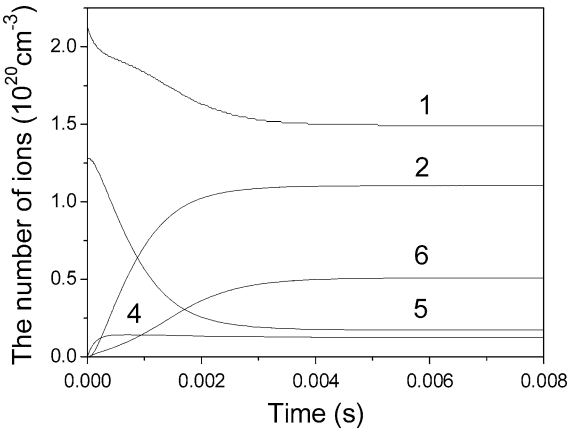

Fig. 6 The dependence of the electron population densities of energy levels of Tm^{3+} and Ho^{3+} on time in TeO_2-WO_3-ZnO glass. The relevant energy levels of Tm^{3+} are (1) $^3H_6$, (2) $^3F_4$ and (4) $^3H_4$ and those of Ho^{3+} are (5) $^5I_8$ and (6) $^5I_7$

intensity. The highest gain can be expected from the tellurite glass doped with 0.5 mol% Tm_2O_3 and 0.15 mol% Ho_2O_3. Comparing gallate glass with the same concentration of Ho_2O_3, tellurite glass has lower pump power threshold and higher gain coefficient.

Conclusion

In summary, we conclude that 2.0-μm emission characteristic and energy transfer of Ho^{3+}-doped tellurite glass sensitized by Tm^{3+} upon excitation of 808 nm laser diode were investigated. Tm^{3+} ions were codoped to populate the $^5I_7$ level of Ho^{3+} and resulted in the intense 2.0-μm emission from tellurite glass. The calculated fluorescence lifetime of the Ho^{3+}: $^5I_7$ level was 3.9 ms, and the emission cross section of the Ho^{3+}: $^5I_7 \rightarrow {}^5I_8$ transition exhibited a maximum

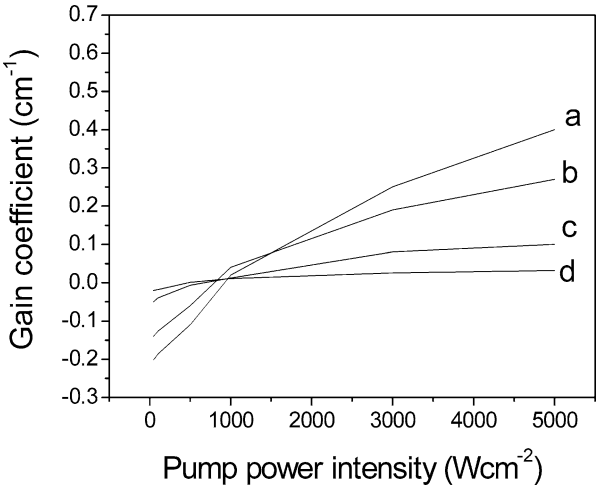

Fig. 7 The dependence of calculated gain coefficients at 2027 nm upon pump power intensity in TeO_2-WO_3-ZnO glasses doped with the Ho_2O_3 concentration of (a) 0.15, (b) 0.1, (c) 0.05 and (d) 0.01 mol% at a fixed Tm_2O_3 concentration of 0.5 mol%

of 9.15×10^{-21} cm^2 at 2027 nm. The coefficients of the forward $Tm^{3+} \rightarrow Ho^{3+}$ energy transfer were approximately 17 times larger than those of the backward $Tm^{3+} \leftarrow Ho^{3+}$ energy transfer. Our result indicated that the highest gain of 2.0-μm emission, due to the transition of Ho^{3+}: $^5I_7 \rightarrow {}^5I_8$, might be achieved from the glass at the rare-earth ion concentration of 0.5 mol% of Tm_2O_3 and 0.15 mol% of Ho_2O_3.

Acknowledgments The authors would like to thank Mr. ZM Feng for technical assistance. This work is jointly supported by NSFC (50472053), NCET (04-0823) and GSTD (2006J1-C0491).

Reference

1. Zou X, Toratani H (1996) Spectroscopic properties and energy transfer in singly-and Tm^{3+}/Ho^{3+} doubly-doped glasses. J Non-Cryst Solids 195:113–124
2. Peng B, Izumitani T (1995) Optical properties, fluorescence mechanisms and energy transfer in Tm^{3+}, Ho^{3+} and Tm^{3+}/Ho^{3+} doped near-infrared laser gasses, sensitized by Yb^{3+}. Opt Mater 4:797–810
3. Shin YB, Lim HT, Choi YG, Kim YS, Heo J (2000) 2.0 μm emission properties and energy transfer between Ho^{3+} and Tm^{3+} in PbO-Bi_2O_3-Ga_2O_3 glasses. J Am Ceram Soc 83(4):787–791
4. Richards BDO, Shen SX, Jha A (2005) Spectroscopy of Tm-Ho co-doped tellurite glass for mid-IR fibre lasers in 1.8–2.2 μm. Proc SPIE 5984(7):1–8
5. Courrol LC, Tarelho LVG, Gomes L, Vieira ND, Cassanjes FC, Messaddeq Y, Ribeiro SJL (2001) Time dependence and energy-transfer mechanisms in Tm^{3+}, Ho^{3+} and Tm^{3+}/Ho^{3+} co-doped alkli niobi μm tellurite glasses sensitized by Yb^{3+}. J Non-Cryst Solids 284:217–222
6. Kim YS, Cho WY, Shin YB, Heo J (1996) Emission characteristics of Ge-Ga-S glasses doped with Tm^{3+}/Ho^{3+}. J Non-Cryst Solids 203:176–181
7. Johson LJ, Boyd GD, Nassau K (1962) Optical maser characteristics of Ho^{3+} in $CaWO_4$. Proc IAE 50:87–90
8. Zhang XL, Wang YZ, Ju YL (2007) Theoretical and experimental study of a single frequency Tm, Ho: YLF Laser. Opt Laser Tech 39(4):782–785
9. Tsuboi T, Murayama H (2006) Energy-transfer upconversion of rare earth ions in ionic crystals: Case of Tm^{3+}/Ho^{3+}-codoped $LiYF_4$ crystals. J Alloys Compd 408–412:680–686
10. Földvári I, Baraldi A, Capelletti R, Magnani N, Sosa RF, Munoz AF, Kappers LA, Watterich A (2007) Optical absorption and luminescence of Ho^{3+} ions in Bi_2TeO_5 single crystal. Opt Mater 29(6):688–696
11. Rai SB, Singh AK, Singh SK (2003) Spectroscopic properties of Ho^{3+} ion doped in tellurite glass. Spectrochimi Acta A 59:3221–3226
12. Judd BR (1962) Optical absorption intensities of rare-earth ions. Phys Rev 127:750–761
13. Ofelt GS (1962) Intensities of crystal spectra and decay of Er^{3+} fluorescence in LaF_3. J Chem Phys 37:511–520
14. Rukmini E, Jayasankar CK (1995) Spectroscopic properties of Ho^{3+} ion in zinc borosulphate glasses and comparative energy level analyses of Ho^{3+} ion in various glasses. Opt Mater 4:529–546
15. Shin YB, Jang JN, Heo J (1995) Mid-infrared light emission characteristics of Ho^{3+}-doped chalcogenide and heavy-metal oxide glasses. Opt Quant Elect 27:379–386
16. Reisfield R, Hormadaly R (1976) Optical intensities of holmiμm in tellurite, calibo, and phosphate glasses. J Chem Phys 64:3207–3212
17. Singh AK, Rai SB, Singh VB (2005) Up-conversion in Ho^{3+} doped tellurite glass. J Alloys Compd 403:97–103
18. Song JH, Heo J, Park SH (2003) Emission properties of PbO-Bi_2O_3-Ga_2O_3 –GeO_2 glasses doped with Tm^{3+} and Ho^{3+}. J Appl Phys 93:9441–9445
19. Lee TH, Heo J (2005) 1.6 μm emission and gain properties of Ho^{3+} in selenide and chalcohalide glasses. J Appl Phys 98:113510
20. Zhang QY, Li T, Jiang ZH (2005) 980 nm laser-diode-excited intense blue upconversion in Tm^{3+}/Yb^{3+}-codoped gallate-bismuth-lead glasses. Appl Phys Lett 87:171911; Zhang QY, Li T (2006) Effects of PbF_2 doping on structure and spectroscopic properties of Ga_2O_3–GeO_2–Bi_2O_3–PbO glasses doped with rare earths. J Appl Phys 90:033510
21. Vila LD, Gomes L, Eyzaguirre CR, Rodriguez E, Cesar CL, Barbosa LC (2005) Time resoled luminescence in (Tm:Ho) doped tellurite glass. Opt Mater 27:1333–1339
22. Spector N, Reisfield R, Boehm L (1977) Eigenstates and radiative transition probabilities for Tm^{3+} ($4f^{12}$) in phosphate and tellurite glasses. Chem Phys Lett 49:49–53
23. ÖZen G, Aydinli A, Cenk S, Sennaroğlu A (2003) Effect of compositon on spontaneous emission probabilities, stimulated emission cross-sections and local environmental of Tm^{3+} in TeO_2-WO_3 glass. J Lumin 101:293–306
24. Press WH, Hu JW, Zhao ZY, Xue YH (2005) Numerical recipes in C++: the art of scientific computing. Publishing House of Electronics Industry, Beijing
25. Volkov EA (1989) Numerical methods. Hemisphere Pub Corp., New York